Metal-Insulator Transitions in Pyrochlore Oxides $Ln_2Ir_2O_7$

Kazuyuki MATSUHIRA*, Makoto WAKESHIMA[1], Yukio HINATSU[1], and Seishi TAKAGI

Faculty of Engineering, Kyushu Institute of Technology, Kitakyushu 804-8550, Japan
[1]*Division of Chemistry, Graduate School of Science, Hokkaido University, Sapporo 060-0810, Japan*

(Received August 4, 2011)

We report the physical properties of $Ln_2Ir_2O_7$ (Ln = Nd, Sm, Eu, Gd, Tb, Dy, and Ho), which exhibit metal-insulator transitions (MITs) at different temperatures. The transition temperature T_{MI} increases with a reduction in the ionic radius of Ln. The ionic radius boundary for MITs in $Ln_2Ir_2O_7$ lies between Ln = Pr and Nd. MITs in $Ln_2Ir_2O_7$ have some common features. They are second-order transitions. Under the field cool condition, a weak ferromagnetic component ($\sim 10^{-3}$ μ_B/f.u.) caused by Ir $5d$ electrons is observed below T_{MI}. The entropy associated with MITs for Ln = Nd, Sm, and Eu is estimated to be 0.47, 2.0, and 1.4 J/K mole, respectively. The change in entropy is much smaller than $2R$ ln 2 [11.5 J /K mole] expected in a magnetic transition due to localized moments of $S = 1/2$. The feature of continuous MITs in $Ln_2Ir_2O_7$ is discussed.

KEYWORDS: metal-insulator transition, pyrochlore oxides, $Nd_2Ir_2O_7$, $Sm_2Ir_2O_7$, $Eu_2Ir_2O_7$,$Gd_2Ir_2O_7$, $Tb_2Ir_2O_7$, $Dy_2Ir_2O_7$, $Ho_2Ir_2O_7$

1. Introduction

In recent years, pyrochlore oxides have been actively researched on account of their structure. These oxides are composed of a network of corner-shared tetrahedra, whose vertices are occupied by spins; these spins may give rise to strong geometrical frustration.[1–6] An important issue that has to be solved is the clarification of how the geometrical frustration influences the ground states of strongly correlated electron systems in three-dimensional triangle-based lattices. In the case of metallic pyrochlore oxides, the frustration originating from the pyrochlore lattice might also lead to novel types of electronic properties. $4d$ and $5d$ transition-metal pyrochlore oxides have recently attracted considerable interest because of their novel transport properties such as the anomalous Hall effect in $Nd_2Mo_2O_7$ and $Pr_2Ir_2O_7$, superconductivity in $Cd_2Re_2O_7$ and AOs_2O_6 (A = K, Rb, and Cs), and the metal-insulator transition (MIT) in $Cd_2Os_2O_7$.[7–14]

In a recent study, we successfully synthesized purified polycrystalline samples of pyrochlore iridates $Ln_2Ir_2O_7$. We observed that $Ln_2Ir_2O_7$ for Ln = Nd, Sm, and Eu exhibits MITs at 36, 117, and 120 K, respectively. [15] In this case, thermal hysteresis and a discontinuous change in the physical properties of pyrochlore iridates were not observed at the MIT temperature

*E-mail address: matuhira@elcs.kyutech.ac.jp

T_{MI}; from this, we concluded that the MITs were second-order transitions. As the ionic radius of Ln reduces, T_{MI} tends to increase. In the case of $Pr_2Ir_2O_7$, no MIT was observed, as it exhibited metallic behavior down to 0.3 K.[16] The ionic radius boundary for MITs in $Ln_2Ir_2O_7$ lies between Ln = Pr and Nd. The electrical conductivity of $Ln_2Ir_2O_7$ depends on the ionic radius of Ln. Similar behavior of the dependence of electrical conductivity on ionic radius is also observed in $Ln_2Mo_2O_7$.[17,18] Since the Ln ion is trivalent, the $(5d)^5$ electrons from Ir^{4+} form an unfilled t_{2g} band. The $4f$ electrons are generally well localized, thus, only the $5d$ electrons contribute to the electrical conductivity. As the ionic radius of Ln reduces, the Ir-O-Ir bond angle decreases, consequently, the t_{2g} bandwidth becomes narrower.[19] Finally, for Ln = Y, a Mott insulator is realized because of the strong electron correlations.[20] In a recent theoretical study, for this insulating state of $Ln_2Ir_2O_7$, the possibility of realizing a topological insulator is discussed.[21] However, the origin of MIT in $Ln_2Ir_2O_7$ is still not clear.

In this paper, we report on the physical properties of higher-quality samples of $Ln_2Ir_2O_7$, where, Ln = Nd, Sm, and Eu. In addition, we obtained high-quality samples of heavy rare-earth pyrochlore iridates for Ln = Gd, Tb, Dy, and Ho. We also report the physical properties of these heavy rare-earth pyrochlore iridates.

2. Experimental Procedure

Polycrystalline samples of $Ln_2Ir_2O_7$ (Ln = Pr, Nd, Sm, Eu, Gd, Tb, Dy, and Ho) were synthesized by a standard solid-state reaction. The mixtures were prepared using rare-earth oxides (99.99% Ln_2O_3 for Ln = Nd, Sm, Eu, Gd, Dy, and Ho; 99.99% for Pr_6O_{11}; 99.99% for Tb_4O_7), IrO_2 (Tanaka Kikinzoku Kogyo) or Ir metal (Tanaka Kikinzoku Kogyo). The molar ratio of Ln to Ir was 1 : 1.1. The mixtures were then pressed into pellets, which were then inserted into a Pt tube and heated at 1423 - 1523 K for about 10 days in a vacuum silica tube with several intermediate grindings. After adding 10 mol% IrO_2, the process was continued for 4 days with several intermediate grindings. The last process was repeated once. The reaction products were identified by powder X-ray diffraction (XRD) measurements. Their XRD patterns indicated a single phase with a cubic pyrochlore structure. From the result of their XRD patterns, we confirmed that the obtained samples are of high quality; the sample of $Sm_2Ir_2O_7$ is that denoted by #2 in our previous paper.[15] The obtained lattice parameters are broadly consistent with the previous results.[1,22]

The electrical resistivity of the obtained samples was measured by a DC four-probe method from 4.2 to 300 K. The thermoelectric power was measured by a differential method using a pair of thermocouples (chromel/Au + 7 at% Fe) from 4.2 to 300 K. DC magnetizations were measured using a SQUID magnetometer (MPMS, Quantum Design, Inc.). Specific heat measurements were performed by a thermal relaxation method (PPMS, Quantum Design, Inc.).

As is reported in ref. 15, we were unable to prepare samples free from impurity phases

by a solid-state reaction in air because of the volatility of IrO_2. Furthermore, their reflection peaks in XRD patterns were much broader. This result indicates that the samples prepared in air have poorer crystallinity or deviate from their stoichiometry. Note that before our study in ref. 15, all polycrystalline samples were prepared by a solid-state reaction in air.[20,22–26]

3. Results and Discussion

3.1 Resistivity

Figure 1 shows the temperature dependence of the electrical resistivities $\rho(T)$ of $Ln_2Ir_2O_7$ for Ln = Pr, Nd, Sm, Eu, Gd, Tb, Dy, and Ho. When Ln is changed from Pr to Dy, $\rho(T)$ at room temperature gradually increases; $\rho(T)$ for Ln = Ho at room temperature is lower than that for Dy.[27] The gradient of $\rho(T)$ at room temperature gradually changes from a positive value to a negative value. For Ln = Pr and Nd, $Ln_2Ir_2O_7$ is metallic. For Ln = Sm, Eu, and Gd, $Ln_2Ir_2O_7$ is semimetallic. For Ln = Tb, Dy, and Ho, $Ln_2Ir_2O_7$ is semiconducting. We found that, for Ln = Nd, Sm, Eu, Gd, Tb, Dy, and Ho, $Ln_2Ir_2O_7$ exhibits MITs at 33, 117, 120, 127, 132, 134, and 141 K, respectively, while $Pr_2Ir_2O_7$ exhibits no MIT down to 0.3 K; it should be noted that T_{MI} forLn = Nd is revised to 33 K.[28,29] Now, although the conductivity of $Ln_2Ir_2O_7$ for Ln = Tb, Dy, and Ho is semiconducting with a small energy gap at room temperature, we have adopted MIT for convenience because a common feature in their transition is observed. T_{MI} increases monotonically as the ionic radius of Ln decreases. The ionic radius boundary for MITs in $Ln_2Ir_2O_7$ lies between Ln = Pr and Nd. For Ln = Gd, Tb, Dy, and Ho, a clear upturn due to MIT is shown in Fig. 1(b). Discontinuities and thermal hysteresis were not observed at approximately T_{MI}, indicating that these MITs are second-order transitions. It should be noted that $\rho(T)$ below T_{MI} continues to increase without saturation on cooling. This implies that MITs in $Ln_2Ir_2O_7$ are not of accidental origin but of essential one.

We then attempted the order estimation of the energy gap in the insulating state from the data. For the data just below T_{MI}, we tried to estimate the energy gap by assuming the equation $\rho(T) = \rho_0 \exp(E_g/T)$, where E_g is the energy gap. The estimated E_g is about 300-600 K; E_g for Ln = Nd, Sm, Eu, Gd, Tb, Dy, and Ho is estimated to be 405, 493, 429, 330, 517, 569, and 463 K, respectively. We found that the energy gap for Ln = Tb, Dy, and Ho increases by about 100-200 K below T_{MI}. These values may roughly correspond to the energy gap, although no systematic change has been confirmed. The band gap in the insulated state is small in comparison with that in $3d$ electron system.[30] Below T_{MI}, $\rho(T)$ cannot be described by the thermal activation conduction form $\rho(T) = \rho_0 \exp(E_g/T)$. In addition, $\rho(T)$ below T_{MI} cannot be expressed in terms of the variable range hopping except for Ln = Eu.[31]Further investigation on the unconventional temperature dependence of resistivity in the insulating state is required to verify the origin.

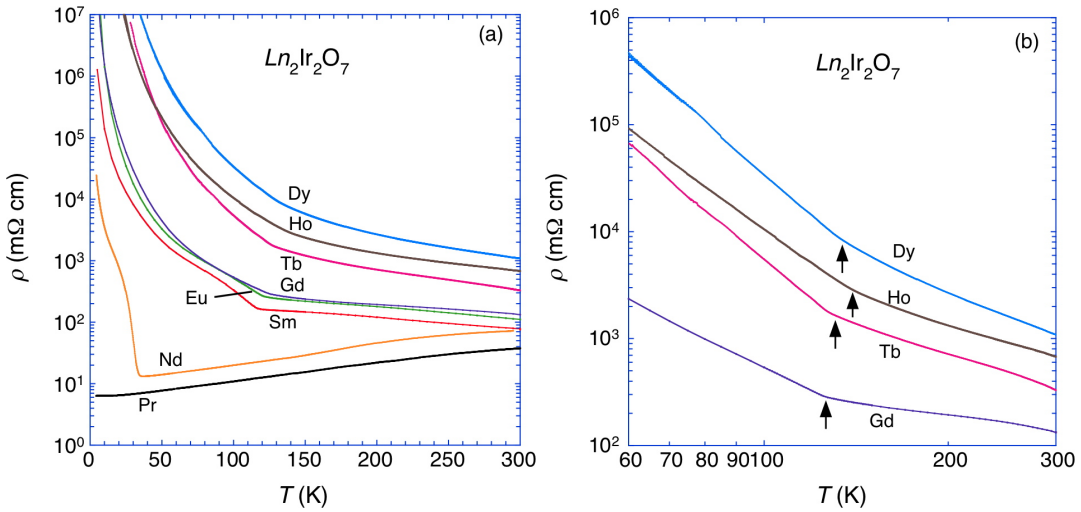

Fig. 1. (a) (Color online) Electrical resistivities of $Ln_2Ir_2O_7$ for Ln = Pr, Nd, Sm, Eu, Gd, Tb, Dy, and Ho. (b) (Color online) Enlarged view of electrical resistivities of $Ln_2Ir_2O_7$ for Ln = Gd, Tb, Dy, and Ho.

3.2 Thermoelectric power

Figure 2 shows the temperature dependences of the thermoelectric powers $S(T)$ of $Ln_2Ir_2O_7$ for Ln = Pr, Nd, Sm, Eu, and Gd. When Ln is changed from Pr to Gd, the sign of $S(T)$ at room temperature changes from negative to positive; this result suggests that the main carrier changes from electron-like for Ln = Pr to hole-like for Ln = Gd. $S(T)$ for Ln = Pr and Nd is negative above 11 K. The sign of $S(T)$ changes to positive below 11 K. The $S(T)$ for Ln = Pr and Nd have broad minima at around 65 and 80 K, respectively. The temperature dependences of the $S(T)$ for Ln = Pr and Nd are quite different from that of a normal metal. The absolute values of the $S(T)$ for Ln = Pr and Nd are also larger than that of a normal metal. $S(T)$ for Ln = Nd bends slightly downward at $T_{\rm MI}$. Below $T_{\rm MI}$, $S(T)$ for Ln = Nd shows a complex temperature dependence on cooling. On the other hand, the $S(T)$ for Ln = Sm, Eu, and Gd are positive. $S(T)$ at room temperature increases when Ln is changed from Sm to Gd. The $S(T)$ for Ln = Sm, Eu, and Gd gradually increase on cooling. Broad maxima for Ln = Sm, Eu, and Gd appear at 150, 175, and 200 K, respectively. These features are consistent with those of the semimetallic behavior of the $\rho(T)$ for Ln = Sm, Eu, and Gd. At $T_{\rm MI}$, the $S(T)$ for Ln = Sm, Eu, and Gd exhibit a clear upturn.

$S(T)$ for Ln = Eu at 300 K (36 μV/K) is larger than that for sample #1 (27 μV/K), as reported in a previous paper.[15] Furthermore, in the first report on the $S(T)$ of $Eu_2Ir_2O_7$ synthesized in air, $S(T)$ (10 μV/K) is much smaller than that of the samples synthesized in a vacuum silica tube.[23] This strong sample dependence on $S(T)$ suggests an influence of the flat-band structure on the pyrochlore lattice. In particular, because $Eu_2Ir_2O_7$ is semimetallic, the carrier density is sensitive to deviations from the stoichiometry.

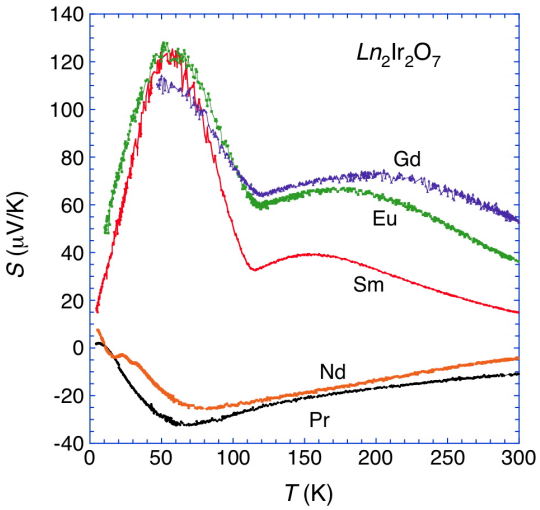

Fig. 2. (Color online) Thermoelectric powers of $Ln_2Ir_2O_7$ for Ln = Pr, Nd, Sm, Eu, and Gd.

3.3 Magnetic susceptibility

Figure 3 shows the magnetic susceptibilities M/H of $Ln_2Ir_2O_7$ for Ln = Nd, Sm, Eu, Gd, Tb, Dy, and Ho; the applied magnetic fields are 1 kOe for Ln = Nd, Sm, Eu, and Gd and 50 G for Ln = Tb, Dy, and Ho. It should be noted that a difference in the M/H measured under the zero-field-cooled (ZFC) and field-cooled (FC) conditions is unexceptionally observed in the MIT of $Ln_2Ir_2O_7$. M/H measured under the ZFC condition show a small peak or a weak kink at T_{MI}. On the other hand, M/H measured under the FC condition shows an upturn at T_{MI} and tends to saturate far below T_{MI}. Although the anomalies in the $\rho(T)$ of $Ln_2Ir_2O_7$ (Ln = Tb, Dy, and Ho) are unclear, there is a clear difference between the M/H measured under ZFC and FC conditions below T_{MI}. Therefore, the anomaly in M/H is a common feature of the MIT of $Ln_2Ir_2O_7$. Hereafter, we will discuss the origin of the anomaly in M/H. The magnetization process at 5 K in $Sm_2Ir_2O_7$ has been reported by Taira *et al.*[26] The magnetization under the FC condition indicates the emergence of very weak ferromagnetic components ($\sim 10^{-3}$ μ_B/f.u.) below T_{MI}. The difference in the M/H measured under the ZFC and FC conditions is attributed to the very weak ferromagnetic components. The present result indicates that the observed emergence of very weak ferromagnetic components is intrinsic. However, it is very difficult to consider the very weak ferromagnetic ordering as the origin of MIT because the observed ferromagnetic moment is very small as magnetic ordering. Therefore, it is reasonable to consider that the emergence of very weak ferromagnetic components is caused by an additional effect. We should explore another possibility as the origin of MIT. A canted antiferromagnetic ordering is speculated as one of the candidates. Lastly, we have pointed out that a difference in the M/H measured under the ZFC and FC conditions is also observed in the MIT of $Cd_2Os_2O_7$ just below T_{MI} = 225 K.[14] Further studies of the magnetic ordered state below T_{MI} are highly desirable.

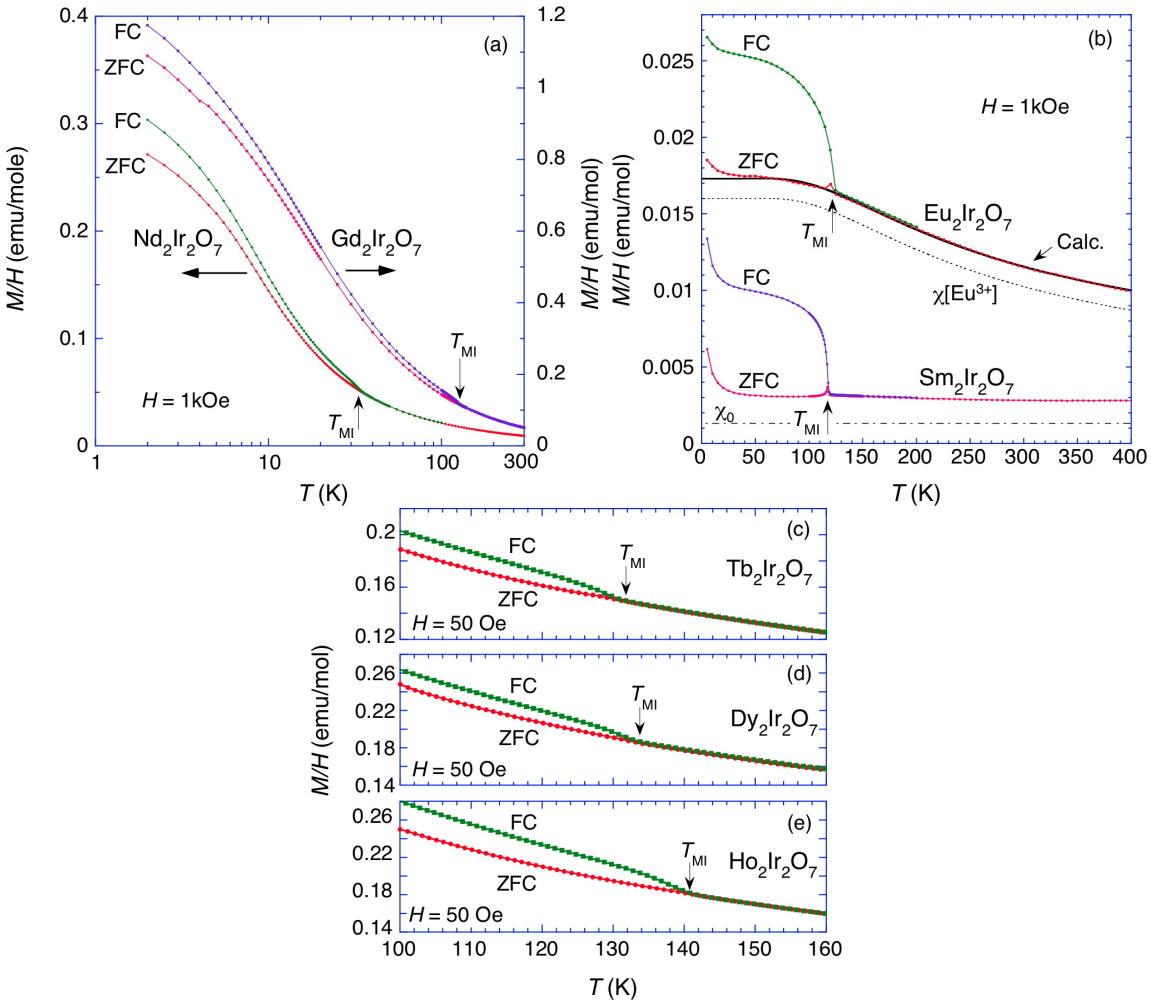

Fig. 3. (a) (Color online) Magnetic susceptibilities M/H of $Nd_2Ir_2O_7$ and $Gd_2Ir_2O_7$ in a magnetic field of 1 kOe. (b) (Color online) M/H of $Sm_2Ir_2O_7$ and $Eu_2Ir_2O_7$ in a magnetic field of 1 kOe. The data of $Sm_2Ir_2O_7$ is the same as that reported in ref. 15. Fitting curve (solid line) for magnetic susceptibility of $Eu_2Ir_2O_7$ above T_{MI}. The dotted line indicates the contribution of the Van Vleck susceptibility due to Eu^{3+} with a spin-orbit coupling constant $\lambda = 375$ K. The dash-dotted line shows a constant contribution $\chi_0 = 1.3 \times 10^{-3}$ emu/mole. M/H in a magnetic field of 50 Oe around T_{MI} for (c) (Color online) Ln = Tb, (d) (Color online) Ln = Dy, and (e) (Color online) Ln = Ho.

Next we will discuss the contribution of the Ln site in the magnetic susceptibility of $Ln_2Ir_2O_7$. In Fig. 3(a), below T_{MI}, the M/H of $Nd_2Ir_2O_7$ under both the FC and ZFC conditions increase up to 2 K. This increase is caused by the magnetic moment of the Nd^{3+} ion as the crystalline electric field (CEF) with the D_{3d} symmetry splits the ground state $J = 9/2$ multiplet in Nd^{3+} into five Kramers doublets. Figure 4(a) shows the reciprocal magnetic susceptibility $(M/H)^{-1}$ of $Nd_2Ir_2O_7$ measured in a magnetic field of 1 kOe. The ZFC data in the temperature range of 10 to 30 K ($< T_{MI}$) is fitted by using the Curie-Weiss (CW) law. It

is known that the magnetic moment of Nd^{3+} in the pyrochlore oxide $Nd_2Mo_2O_7$ has a $\langle 111 \rangle$ local Ising anisotropy axis.[7] Assuming $\langle 111 \rangle$ local Ising anisotropy, we obtained an effective moment $\mu_{\rm eff} = 2.73\ \mu_{\rm B}$ and a CW temperature $\Theta_{\rm CW} = -3.0$ K by CW fitting. The estimated $\mu_{\rm eff}$ is close to that of the pyrochlore oxide $Nd_2Sn_2O_7$ ($\mu_{\rm eff} = 2.63\ \mu_{\rm B}$), where the Sn^{4+} ion is non-magnetic and shows an AFM ordering at 0.91 K.[32] The deviation from the CW law becomes clear below 8 K. The increase in M/H is suppressed to below 8 K.

Next, the M/H of $Sm_2Ir_2O_7$ exhibits a very weak temperature dependence above $T_{\rm MI}$ [Fig. 3(b)]. Both the ZFC and FC results indicate that M/H increases below 40 K. This increase in the M/H of $Sm_2Ir_2O_7$ is caused by the magnetic moment of the Sm^{3+} ion; this is because the CEF with the D_{3d} symmetry splits the ground state $J = 5/2$ multiplet in Sm^{3+} into three Kramers doublets. Further study of the CEF states is needed in order to characterize the magnetic properties of $Sm_2Ir_2O_7$.

Next, the M/H of $Eu_2Ir_2O_7$ exhibits Van Vleck paramagnetism at low temperatures as Eu^{3+} has the ground state $J = 0$ multiplet [Fig. 3(b)]. In the case of Eu^{3+} ($4f^5$), the energy splitting between the ground state ($J = 0$) and the 1st excited states ($J = 1$) is known to be $\sim$ 300 K. This energy splitting corresponds to the spin-orbit coupling constant λ. The equation for the $\chi(T)$ of Eu^{3+} ions was obtained by Van Vleck; in the equation, the CEF effect is not considered.[33] Therefore, the slight upturn in the M/H of $Eu_2Ir_2O_7$ below 10 K is caused by a small amount of magnetic impurity [Fig. 3(b)]. By using the Van Vleck equation, we tried to reproduce the M/H of $Eu_2Ir_2O_7$ above $T_{\rm MI}$ using λ and a constant (χ_0) as fitting parameters. Then, we obtained a good fit for the parameters of $\lambda = 375$ K and $\chi_0 = 1.3 \times 10^{-3}$ emu/mol [see Fig. 3(b)]. This result suggests that the $5d$ electrons from Ir are not localized above $T_{\rm MI}$. A low carrier from the t_{2g} band, indicating semimetallic behavior, shows Pauli paramagnetism above $T_{\rm MI}$. Note that this value of Pauli paramagnetism is close to that estimated in $Pr_2Ir_2O_7$.[16] Since $Pr_2Ir_2O_7$ is metallic, the carrier density is much higher than that of $Eu_2Ir_2O_7$. Therefore, it is speculated that the Pauli paramagnetism from $5d$ electrons in $Eu_2Ir_2O_7$ is enhanced by an electron correlation effect.

Next, in Fig. 3(a), the M/H of $Gd_2Ir_2O_7$ under both the FC and ZFC conditions increase up to 2 K. This increase is caused by the magnetic moment of the Gd^{3+} ion ($^8S_{7/2}$ ground state), which exhibits magnetic isotropy. Figure 4(b) shows the reciprocal magnetic susceptibility $(M/H)^{-1}$ of $Gd_2Ir_2O_7$ measured in a magnetic field of 1 kOe. Above $T_{\rm MI}$, the $(M/H)^{-1}$ of $Gd_2Ir_2O_7$ is well followed by the CW law. Assuming the CW law in the temperature range of 150-300 K, we obtained $\Theta_{\rm CW} = -7.9$ K and $\mu_{\rm eff} = 7.91\ \mu_{\rm B}$. The estimated $\mu_{\rm eff}$ is very close to 7.94 $\mu_{\rm B}$ for the $^8S_{7/2}$ ground state of the Gd^{3+} ion. In fact, $\mu_{\rm eff} = 7.96\mu_{\rm B}$ in the highly frustrated pyrochlore magnet $Gd_2Sn_2O_7$ (where the Sn^{4+} ion is nonmagnetic and shows AFM ordering at 1.0 K) is consistent with the above-mentioned value.[32,34] If $5d$ electrons from Ir^{4+} show a localized magnetism of $S = 1/2$, $\mu_{\rm eff}$ is expected to be 8.124 $\mu_{\rm B}$. Because the observed

value is much smaller than the expected value, we should consider the itinerant magnetism of $5d$ electrons above $T_{\rm MI}$. The negative $\Theta_{\rm CW}$ suggests an AFM correlation between Gd moments. However, the M/H under both FC and ZFC conditions show CW behavior below $T_{\rm MI}$. Therefore, Gd moments have no long-range ordering at least down to 2 K.

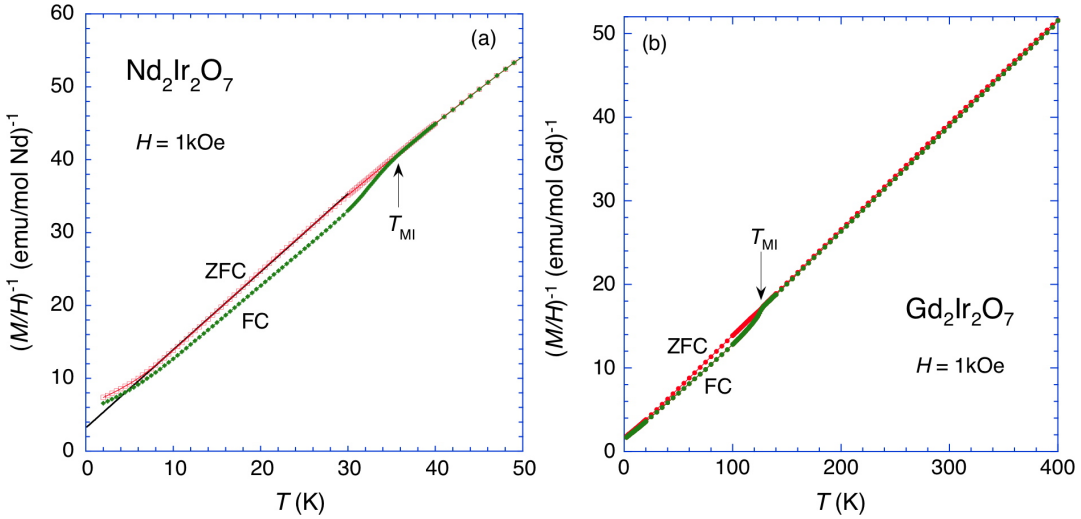

Fig. 4. (a) (Color online) Reciprocal magnetic susceptibility $(M/H)^{-1}$ of $Nd_2Ir_2O_7$ below 50 K. The solid line shows a fitting for ZFC data in the temperature range of 10 to 30 K. (b) (Color online) Reciprocal magnetic susceptibility $(M/H)^{-1}$ of $Gd_2Ir_2O_7$.

3.4 Specific heat

Figure 5(a) shows the C/T of $Nd_2Ir_2O_7$ below 40 K. An anomaly due to MIT is observed at $T_{\rm MI}$, which is consistent with the anomalies in the resistivity, thermoelectric power, and magnetization. The entropy associated with the MIT will be discussed later. Next, Fig. 5(b) shows the C/T of $Nd_2Ir_2O_7$ below 25 K. C/T shows a broad peak at 4 K and a shoulder at 1 K. From the entropy variation, this broad peak is caused by the CEF ground state doublet in Nd^{3+}. Then, we can fit the data using the Schottky specific heat of two levels with energy splitting Δ = 13 K; the lattice contribution estimated from the data of $Eu_2Ir_2O_7$ is also considered in this fitting. A good fitting is obtained above 5 K. Because Nd^{3+} is a Kramers ion, the splitting is caused by the internal field due to a *d-f* interaction. This suggests the appearance of an internal field due to MIT below $T_{\rm MI}$. A slight deviation below 5 K may be caused by the influence of a weak interaction between Nd moments.

Figure 6 shows the C/T of $Eu_2Ir_2O_7$ and $Sm_2Ir_2O_7$. A sharp anomaly in both compounds is observed at $T_{\rm MI}$, which confirms a bulk transition. An upturn in the C/T of Ln = Sm observed below 7 K is attributed to the tail of a Schottky anomaly due to the CEF ground state doublet in Sm^{3+}, as previously reported.[15] Indeed, there is no upturn in the C/T of

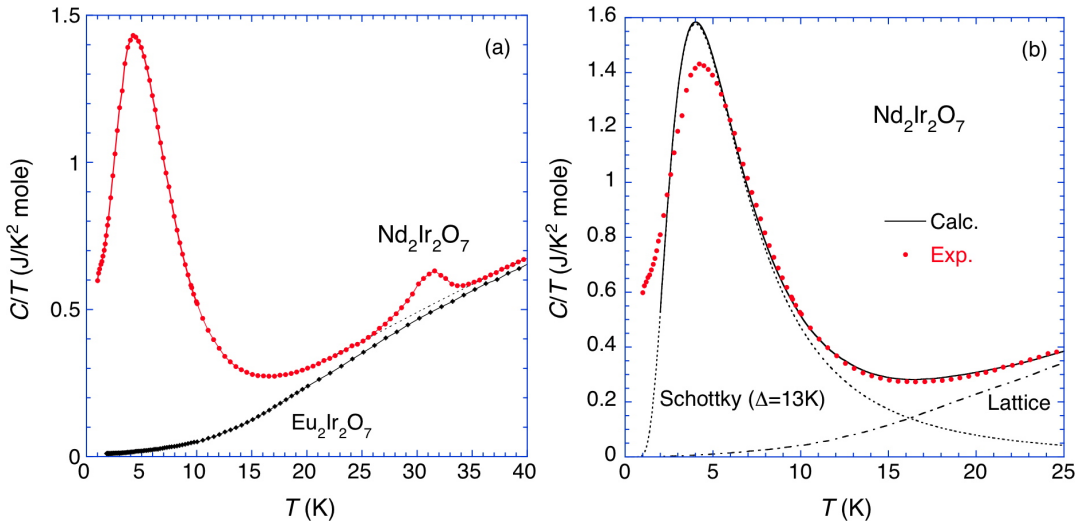

Fig. 5. (a)(Color online) Specific heat divided by temperature C/T of $Nd_2Ir_2O_7$. The broken line shows a smooth polynomial fitted to the data outside the region of the anomaly. (b)(Color online) Analysis of specific heat divided by temperature C/T of $Nd_2Ir_2O_7$ below 25 K. The broken line shows the Schottky specific heat with energy splitting $\Delta = 13$ K. The dash-dotted line shows the lattice contribution estimated from the data of $Eu_2Ir_2O_7$. The solid line shows the sum of these contributions.

Ln = Eu at low temperatures because Eu^{3+} has the ground state multiplet of $J = 0$. The $C(T)$ of $Eu_2Ir_2O_7$ between 1.8 and 9 K can be well fitted by $C/T = \alpha + \beta T^2$ (the Debye T^3 law); the Debye temperature $\Theta_D = (12\pi^4 R_g n/5\beta)^{1/3}$, where R_g is the gas constant and $n = 11$. In this manner, we obtained $\alpha = 8.6$ mJ/K^2 mole and $\Theta_D = 374$ K. Θ_D is slightly larger than the previous value ($\Theta_D = 304$ K).[24] Here, note that α does not correspond to an electronic specific heat coefficient because the electrical conductivity for Ln = Eu below 10 K extends beyond 10^6 mΩ cm. The result means that $C(T)$ has a small T-linear contribution in the insulator. Firstly, the contribution of magnon associated with the AFM order induced by MIT can be considered at low temperatures. However, the T-linear contribution in $C(T)$ is known to be attributed to spin wave excitations for one-dimensional antiferromagnets; it is difficult for the pyrochlore lattice to induce a T-linear contribution. As another possible origin for T-linear contribution in $C(T)$ in the insulating state, Anderson localization may be considered.[35] Further investigation is required to reveal the origin of the T-linear contribution.

Now we will discuss the Ln dependence of the entropy associated with the MIT (ΔS). To estimate ΔS, a smooth polynomial was fitted to the data outside the region of the anomaly; these fitting lines (broken line) for Ln =Nd, Sm, and Eu are shown in Figs. 5(a), 6(a), and 6(b), respectively. The background contribution was subtracted from the raw data; the electronic portions of the C/T ($\Delta C/T$) for Ln =Sm and Eu are shown in the inset. By integrating $\Delta C/T$, we obtained $\Delta S = 0.47$, 2.0, and 1.4 J/K mole for Ln = Nd, Sm, and Eu, respectively.

ΔS is much smaller than $2R$ ln 2. If we assume that a localized $5d$ electron from Ir^{4+} ions with $S = 1/2$ causes a conventional magnetic transition, we can expect a change in entropy of $2R$ ln 2 = 11.5 J/K mole. The reduction in the amount of change in entropy is considered to be caused by a short-range ordering due to frustration or a reduction in magnetic moment due to the itinerancy of $5d$ electrons. Next, recently, the Raman scattering spectra of $Ln_2Ir_2O_7$ for Ln = Nd, Sm, and Eu have been measured.[36] Below T_{MI}, new peaks appear for Ln = Sm and Eu, but no remarkable change is seen for Ln = Nd. The result indicates that $Sm_2Ir_2O_7$ and $Eu_2Ir_2O_7$ accompany a structural change with MIT, but this does not occur with $Nd_2Ir_2O_7$. Therefore, the ΔS for Ln = Sm and Eu involve the lattice contribution. Indeed, ΔS for Ln = Nd is smaller than those for Ln = Sm and Eu. If we consider this ΔS in Ln = Nd to be caused by only the electronic contribution without the lattice contribution, we can estimate the electronic specific heat coefficient above T_{MI} $\gamma = 14$ mJ/K^2 mole by the relation $\gamma = \Delta S/T_{MI}$. As $Sm_2Ir_2O_7$ and $Eu_2Ir_2O_7$ are both semimetallic from the behaviors of their $\rho(T)$ and $S(T)$, it is speculated that the γ for Ln = Sm and Eu are smaller than that for Ln = Nd.

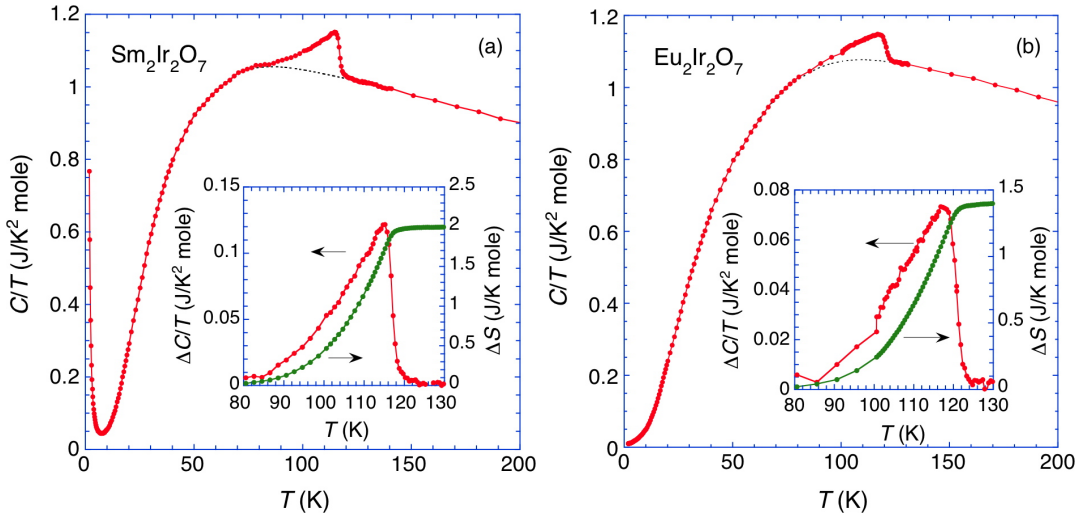

Fig. 6. (Color online) Specific heat divided by temperature, C/T, of (a) $Sm_2Ir_2O_7$ and (b) $Eu_2Ir_2O_7$. The broken line shows a smooth polynomial fitted to the data outside the region of the anomaly. The inset shows the electronic portion of C/T ($\Delta C/T$) obtained, as described in the text. The inset also shows the entropy ΔS estimated from $\Delta C/T$.

3.5 Phase diagram

Figure 7 shows the phase diagram of $Ln_2Ir_2O_7$, which is based on the Ln^{3+} ionic radius dependence of T_{MI}; the ionic radius of Ln^{3+} is for an 8-coordination-number site. T_{MI} monotonically increases as the ionic radius of Ln^{3+} decreases. Obviously, T_{MI} does not depend on the de Gennes factor $(g_J - 1)^2 J(J+1)$ or the magnetism of Ln^{3+}. This MIT is not associated

with the magnetic ordering of Ln^{3+}. For $T > T_{\rm MI}$, Ln = Pr and Nd are metallic. Then, Ln = Sm, Eu and Gd are semimetallic and Ln = Tb, Dy, and Ho are semiconducting. Ln = Pr is a unique metal located near the critical point of MIT. In this figure, the extrapolation between Ln = Nd and Pr is based on a recent result for resistivity in the solid solution $(Pr_{1-x}Nd_x)_2Ir_2O_7$.[37] From the result, the substitution of Pr by 20% Nd leads to MIT at around 3 K; below $T_{\rm MI}$, the increasing resistivity in this sample is suppressed, and resistivity reaches a finite value at lower temperatures.

Next, we discuss the phase diagram of $Ln_2Ir_2O_7$ in comparison with that of other rare-earth pyrochlore oxides. The phase diagrams of $Ln_2Mo_2O_7$ (Mo^{4+}: $(4d)^2$) have already been reported.[38–40] Now, we point out the difference in the phase diagram between Ir and Mo pyrochlore oxides. As is described in the introduction, as the ionic radius of Ln^{3+} decreases, the electrical conductivity in $Ln_2Mo_2O_7$ becomes semiconducting. Interestingly, the magnetic transition of $Ln_2Mo_2O_7$ goes from the spin glass insulating state (Ln = Gd, Tb, Dy, and Ho) to the ferromagnetic metallic state (Ln = Eu, Sm, and Nd) as the ionic radius of Ln^{3+} increases; the ferromagnetic transition comes from $4d$ electrons. Although the spin glass transition temperature $T_{\rm g}$ is independent of Ln ($T_{\rm g} \sim 20$ K), the ferromagnetic transition temperature increases as the ionic radius of Ln^{3+} increases. In addition, semiconducting $Ln_2Ru_2O_7$ (Ru^{4+}: $(4d)^4$) shows the frustrated AFM transition originating from $4d$ electrons.[41] The Néel temperature $T_{\rm N}$ monotonically increases from $T_{\rm N}$ = 84 K for Ln = Yb to $T_{\rm N}$ = 160 K for Ln = Pr as the ionic radius of Ln^{3+} increases. The present result shows that the magnetic transition (or MIT) in $Ln_2Ir_2O_7$ decreases as the ionic radius of Ln^{3+} increases. Then, the opposite dependence of the ionic radius of Ln^{3+} on the magnetic transition temperature is realized in $Ln_2Ir_2O_7$. It is speculated that the difference in their phase diagrams is due to the feature of the $5d$ electron system, which has a strong spin-orbit interaction and a reduced on-site Coulomb repulsion in comparison with the $4d$ electron system.[21] Further theoretical study is needed to understand this phase diagram in $Ln_2Ir_2O_7$.

4. Conclusions

We report the physical properties (resistivity, thermoelectric power, magnetization, and specific heat) of $Ln_2Ir_2O_7$ for Ln = Nd, Sm, Eu , Gd, Tb, Dy, and Ho. $Ln_2Ir_2O_7$ for Ln = Nd, Sm, and Eu show MITs at 33, 117, and 120 K, respectively. In this study, we revealed that $Ln_2Ir_2O_7$ for Ln = Gd, Tb, Dy, and Ho exhibit MITs at 127, 132, 134, and 141 K, respectively. These MITs in $Ln_2Ir_2O_7$ has some common features: They are second-order transitions since no thermal hysteresis or no discontinuous change in their physical properties is observed at $T_{\rm MI}$. Under the FC condition, a weak ferromagnetic component ($\sim 10^{-3}$ $\mu_{\rm B}$/f.u.) caused by $5d$ electrons from Ir is observed below $T_{\rm MI}$. The entropy associated with MIT supports the notion that this system above $T_{\rm MI}$ is a $5d$ itinerant electron system. The analysis of the specific heat of $Nd_2Ir_2O_7$ reveals that an internal field due to the *d-f* interaction affects the splitting

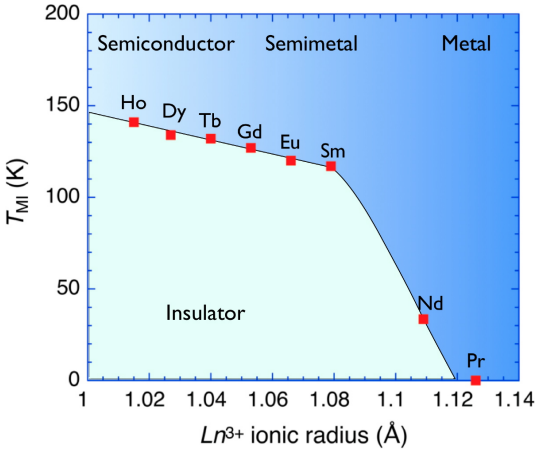

Fig. 7. (Color online) Phase diagram of $Ln_2Ir_2O_7$ based on Ln^{3+} ionic radius dependence of T_{MI}.

of the Kramers ground state doublet below T_{MI}. Furthermore, we have obtained the phase diagram of $Ln_2Ir_2O_7$. The present result shows that T_{MI} in $Ln_2Ir_2O_7$ decreases as the ionic radius of Ln^{3+} increases. Further experimental and theoretical studies are necessary to clarify the origin of MITs in $Ln_2Ir_2O_7$.

Acknowledgments

We would like to thank Z. Hiroi, T. Hasegawa, M. Udagawa, Y. Motome, L. Balents, H. Takagi, and H. Harima for their helpful discussions. Some of the XRD measurements were performed at the Center for Instrumental Analysis at the Kyushu Institute of Technology. This work was supported by a Grant-in-Aid for Scientific Research on Priority Areas "Novel States of Matter Induced by Frustration" (No.19052005) and Grants-in-Aid for Scientific Research on Innovation Areas "Heavy Electrons" (No. 21102518). This research was partly supported by a Grant-in-Aid for Young Scientists (B) (No.17740234) and a Grant-in-Aid for Scientific Research (C) (No. 40312342) from MEXT, Japan.

References

1) M. A. Subramanian, G. Aravamudan, and G. V. Subba Rao: Prog. Solid State Chem. **15** (1983) 55.
2) B. D. Gaulin, J. N. Reimers, T. E. Mason, J. E. Greedan, and Z. Tun: Phys. Rev. Lett. **69** (1992) 3244.
3) M. J. P. Gingras, C. V. Stager, N. P. Raju, B. D. Gaulin, and J. E. Greedan: Phys. Rev. Lett. **78** (1997) 947.
4) H. J. Harris, S. T. Bramwell, D. F. McMorrow, T. Zeiske, and K. W. Godfrey: Phys. Rev. Lett. **79** (1997) 2554.
5) K. Matsuhira, Z. Hiroi, T. Tayama, S. Takagi, and T. Sakakibara: J. Phys.: Condens. matter **14** (2002) L559.
6) C. Castelnovo, R. Moessner, and S. L. Sondhi: Nature **451** (2008) 42.
7) Y. Taguchi, Y. Oohara, H. Yoshizawa, N. Nagaosa, and Y. Tokura: Science **291** (2001) 2573.
8) Y. Machida, S. Nakatsuji, Y. Maeno, T. Tayama, T. Sakakibara, and S. Onoda: Phys. Rev. Lett. **99** (2007) 037203.
9) M. Hanawa, Y. Muraoka, T. Tayama, T. Sakakibara, J. Yamaura, and Z. Hiroi: Phys. Rev. Lett. **87** (2001) 187001.
10) S. Yonezawa, Y. Muraoka, Y. Matsushita, and Z. Hiroi: J. Phys.: Condens. Matter **16** (2004) L9.
11) S. Yonezawa, Y. Muraoka, Y. Matsushita, and Z. Hiroi: J. Phys. Soc. Jpn. **73** (2004) 819.
12) S. Yonezawa, Y. Muraoka, and Z. Hiroi: J. Phys. Soc. Jpn. **73** (2004) 1655.
13) A. W. Sleight, J. L. Gillson, J. F. Weiher, and W. Bindloss: Solid State Commun. **14** (1974) 357.
14) D. Mandrus, J. R. Thompson, R. Gaal, L. Forro, J. C. Bryan, B. C. Chakoumakos, L. M. Woods, B. C. Sales, R. S. Fishman, and V. Keppens: Phys. Rev. B **63** (2001) 195104.
15) K. Matsuhira, M. Wakeshima, R. Nakanishi, T. Yamada, A. Nakamura, W. Kawano, S. Takagi, and Y. Hinatsu: J. Phys. Soc. Jpn. **76** (2007) 043706.
16) S. Nakatsuji, Y. Machida, Y. Maeno, T. Tayama, T. Sakakibara, J. van Duijn, L. Balicas, J. N. Millican, R. T. Macaluso, and J. Y. Chan: Phys. Rev. Lett. **96** (2006) 087204.
17) N. Ali, M. P. Hill, and S. Labroo: J. Solid State Chem. **83** (1989) 178.
18) I. Kézsmárki, N. Hanasaki, D. Hashimoto, S. Iguchi, Y. Taguchi, S. Miyasaka, and Y. Tokura: Phys. Rev. Lett. **93** (2004) 266401.
19) H.-J. Koo, M.-H. Whangbo, and B. J. Kennedy: J. Solid State Chem. **136** (1998) 269.
20) H. Fukazawa and Y. Maeno: J. Phys. Soc. Jpn. **71** (2002) 2578.
21) D. Pesin and L. Balents: Nat. Phys. **6** (2010) 376.
22) D. Yanagishima and Y. Maeno: J. Phys. Soc. Jpn. **70** (2001) 28.
23) R. J. Bouchard and J. L. Gillson: Mater. Res. Bull. **6** (1971) 669.
24) K. Blacklock and H. K. White: J. Chem. Phys. **72** (1980) 2191.
25) C. L. Chien and A. W. Sleight: Phys. Rev. B **18** (1978) 2031.
26) N. Taira, M. Wakeshima, and Y. Hinatsu: J. Phys.: Condens. Matter **13** (2001) 5527.
27) It becomes difficult to prepare a sample in the case of a heavy rare-earth element.
28) Instead, we have confirmed the drop anomaly in $\rho(T)$ at 0.75 K.
29) In our previous study, T_{MI} for Ln = Nd was determined to be 36 K by evaluating the upturn of resistivity. However, we found that a sharp anomaly in specific heat is observed at 33 K in the

present sample; the specific heat data is shown in Fig. 5(a). Therefore, we concluded that $T_{\rm MI}$ for Ln = Nd is 33 K. The resistivity of $Nd_2Ir_2O_7$ shows a slight upturn just above $T_{\rm MI}$ = 33 K, which is affected by the fluctuation in MIT.

30) N. F. Mott: *Metal-Insulator Transitions* (Taylor & Francis, London, 1990) Chap. 6.

31) For $Eu_2Ir_2O_7$, the temperature dependence of $\ln\rho \propto T^{-1/4}$ is observed below 60 K.

32) K. Matsuhira, Y. Hinatsu, K. Tenya, H. Amitsuka and T. Sakakibara: J. Phys. Soc. Jpn. **71** (2002) 1576.

33) J. H. Van Vleck: *The Theory of Electric and Magnetic Susceptibilities* (Oxford University Press, London, 1932) p. 245.

34) P. Bonville, J. A. Hodges, M. Ocio, J. P. Sanchez, P. Vulliet, S. Sosin, and D. Braithwaite: J. Phys.: Condens. Matter **15** (2003) 7777.

35) W. P. Anderson: Phys. Rev. **109** (1958) 1492.

36) T. Hasegawa, N. Ogita, K. Matsuhira, S. Takagi, M. Wakeshima, Y. Hinatsu, and M. Udagawa: J. Phys.: Conf. Series **200** (2010) 012054.

37) K. Kuroda: Graduation Thesis, Faculty of Engineering, Kyushu Institute of Technology, Kitakyushu, Japan (2010) [in Japanese].

38) T. Katsufuji, H. Ẏ. Hwang and S.-W. Cheng: Phys. Rev. Lett. **84** (2000) 1998.

39) Y. Moritomo, Sh. Xu, A. Machida, T. Katsufuji, E. Nishibori, M. Takata, M. Sakata and S.-W. Cheng: Phys. Rev. B **63** (2001) 144425.

40) N. Hanasaki, K. Watanabe, T. Ohtsuka, I. Kézsmárki, S. Iguchi, S. Miyasaka, and Y. Tokura: Phys. Rev. Lett. **99** (2007) 086401.

41) M. Ito, Y. Yasui, M. Kanada, H. Harashima, S. Yoshii, K. Murata, M. Sato, H. Okumura, and K. Kakurai: J. Phys. Chem. Solids **62** (2001) 337.